small
NANO MICRO

Nanorods

Facile Synthesis of Luminescent $AgInS_2$–ZnS Solid Solution Nanorods

Xuyong Yang, Yuxin Tang, Swee Tiam Tan, Michel Bosman, Zhili Dong, Kheng Swee Leck, Yun Ji, Hilmi Volkan Demir, and Xiao Wei Sun**

Semiconductor nanorods (NRs) are of great interest for both scientific fundamental research and technological applications owing to their collective optical, electronic and magnetic properties, such as linearly polarized emission,[1–3] higher photon absorption cross-section,[4] stronger electric dipoles,[5,6] and efficient one-dimensional electrical transport,[7] which are related to their anisotropic shape. Over the past few years, a fine control over single-component semiconductor nanorods has been achieved by colloidal chemistry routes.[8–18] However, the growth of multicomponent nanorods has been relatively less developed. This is mainly due to the distinct material components characterized with different physical properties, surface chemistry and morphologies.[19] The study of multicomponent nanoparticles, consisting of two or more components within each particle, is important both for creating multifunctional nanomaterials and for controlling electronic coupling between nanoscale units.[14] Recently, great development has been made in the multicomponent nanorods in heterostructures,[20–26] leading to revolutionary applications in many fields such as catalysis, photovoltaic devices, and sensors. For example, Manna et al.[25] reported the synthesis of CdSe/CdS/ZnS double shell nanorods with high photoluminescence efficiency biolabeling probes for cell labeling applications. Very recently, highly emissive CdSe/CdS rod in rod core/shell heterostructure with strong linear polarization has been prepared by Banin and co-workers using a seeded-growth approach for potential optical and optoelectronic application.[20] Despite the significant advancements in multicomponent semiconductor heterostructured nanorods, little progress has been made in the solid solution counterparts. Solid solutions possess a homogeneous crystalline structure,[27–32] in which one or more kinds of atoms or molecules may be partly substituted without changing the underlying structure. Semiconductor solid solution nanomaterials[33] with tunable electronic structures are of particular interest because of the effective combination of two or more distinct semiconducting components in one single nanostructure. However, unlike heterostructures, there are no obvious heterointerfaces in solid solutions, and it is more difficult to achieve the morphology and size control. Thus there have been only few reports in the literatures on the synthesis of semiconductor solid solution mircospheres[34] and nanocages,[35] let alone the orientation growth of semiconductor solid solutions, which requires advanced growth control.

On the other hand, currently luminescent semiconductor nanoparticles (quantum dots, nanowires, nanorods, etc.) are primarily based on the cadmium cation-based materials with intrinsic toxicity, limiting the range of their uses for environmentally-friendly applications.[36–47] To date, the synthesis of I–III–VI semiconductor nanoparticles such as $CuInS_2$ and $AgInS_2$ has been intensively investigated due to their low intrinsic toxicity.[48–53] Among them, the $AgInS_2$-ZnS solid solutions consisting of ZnS with a wide band gap

X. Y. Yang, Dr. S. T. Tan, K. S. Leck, Y. Ji, Prof. H. V. Demir, Prof. X. W. Sun
Luminous! Center of Excellence for
Semiconductor Lighting and Displays, School of
Electrical and Electronic Engineering
Nanyang Technological University
Nanyang Avenue, Singapore 639798, Singapore
E-mail: hvdemir@ntu.edu.sg; EXWSun@ntu.edu.sg

Y. X. Tang, Prof. Z. L. Dong
School of Materials Science and Engineering
Nanyang Technological University
Nanyang Avenue, Singapore 639798, Singapore

Dr. M. Bosman
Institute of Materials Research and Engineering
A* STAR (Agency for Science
Technology and Research)
3 Research Link, Singapore 117602, Singapore

DOI: 10.1002/smll.201202656

Prof. H. V. Demir
School of Physical and Mathematical Sciences
Nanyang Technological University
Nanyang Avenue, Singapore 639798, Singapore

Prof. H. V. Demir
Department of Electrical and Electronics Engineering
Department of Physics
UNAM–Institute of Materials Science
and Nanotechnology
Bilkent University
Bilkent, Ankara, 06800, Turkey

Prof. X. W. Sun
Department of Applied Physics
College of Science
and Tianjin Key Laboratory of Low-Dimensional Functional Material
Physics and Fabrication Technology
Tianjin University
Tianjin 300072, China

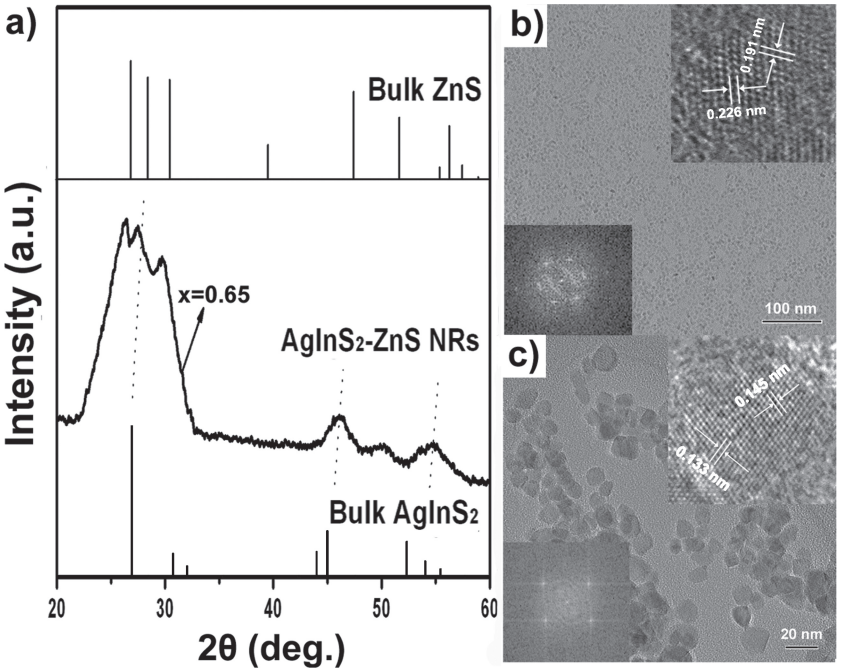

Figure 1. (a) XRD patterns of $AgInS_2$-ZnS solid solution nanorods prepared by decomposition of $(AgIn)_xZn_{2(1-x)}(S_2CN(C_2H_5)_2)_4$ (x = 0.65). Reference patterns of bulk ZnS and $AgInS_2$ are also shown. TEM images of (b) pure ZnS (x = 0) nanoparticles and (c) pure $AgInS_2$ (x = 1) nanoparticles.

(E_g = 3.8 eV) and $AgInS_2$ with a narrow band gap (E_g = 1.80 eV) exhibit appealing optical properties including tunable emission spectrum, large absorption coefficient and high quantum efficiency, offering great potential as an alternative for cadimium-based materials.[54–57] A pioneer work on the preparation of $AgInS_2$-ZnS solid solution nanoparticles was reported by Torimoto's group where the $AgInS_2$-ZnS solid solution nanoparticles with excellent luminescence properties were successfully synthesized by a thermal decomposition of precursor of $(AgIn)_xZn_{2(1-x)}$(DDTC) in N_2 atmosphere.[55] However, the resulting particles were irregular and the yield was low. Since the size, shape and structure of semiconductors are vital parameters for their physical and chemical properties, developing efficient methods for controlled synthesis of $AgInS_2$-ZnS solid solutions is of significant importance for their further applications.

Herein, we report the facile synthesis of $AgInS_2$-ZnS solid solution nanorods by a single-step one-pot solvothermal method, which both enables size control and allows for emission spectrum tunability with molar concentration. These well-dispersed $AgInS_2$-ZnS solid solution nanorods exhibit excellent photoluminescence emission. The anisotropic growth mechanism for $AgInS_2$-ZnS solid solution nanorods has been investigated in detail by manipulating their growth kinetics. In addition, we found that the chemical composition of $AgInS_2$-ZnS solid solutions plays an important role in the process of nanorod formation and the uniform nanorods were only obtained when the mole fraction of $AgInS_2$ in solid solutions lies between 38% and 48%.

In a typical synthesis, 50 mg of $(AgIn)_xZn_{2(1-x)}(S_2CN(C_2H_5)_2)_4$ was added into a solvent made of 10 mmol of OA, 10 mmol of ODA, and 20 mmol of ODE in a three-necked flask at room temperature. The slurry was then heated to 100 °C to remove water and oxygen with vigorous magnetic stirring under vacuum to form an optically transparent solution. Subsequently, the solution was heated to a temperature to 200 °C for 30 min under Ar atmosphere. After cooling to a room temperature, the resulting nanorods were precipitated with excess ethanol and then washed with ethanol and drying. The as-prepared solid solution nanorods were easily re-dispersed in various nonpolar organic solvents (e.g., chloroform). The precursor $(AgIn)_xZn_{2(1-x)}(S_2CN(C_2H_5)_2)_4$ was prepared using the reported method.[55]

The crystal structure of the resulting $AgInS_2$-ZnS solid solution nanorods was investigated by X-ray powder diffraction (XRD) with Cu Kα radiation. As shown in **Figure 1**a, all of the peaks match those of bulk hexagonal ZnS (no. JCPDS 05-0492), and the sample therefore does not contain other crystal phases, e.g., Ag_2S or In_2S_3, except for $AgInS_2$ (though there is a peak at around 40° for the bulk wurtzite ZnS, there is no such peak for nanosized wurtzite ZnS). It can be seen that each peak is shifted to a lower angle compared to that of ZnS because of the presence of $AgInS_2$ and the peak positions lie between the corresponding peaks of bulk hexagonal ZnS and tetragonal $AgInS_2$. These facts indicate that the resulting nanorods were not a mixture of ZnS and $AgInS_2$ but a $AgInS_2$-ZnS solid solution, which is consistent with a previous report;[55] however, in our case, ZnS is hexagonal not cubic. The solid solution nanorod composition of hexagonal ZnS and tetragonal $AgInS_2$ was further confirmed by transmission electron microscopy (TEM; Figure 1b,c). The low magnification TEM images of pure ZnS and $AgInS_2$ samples synthesized under the same reaction conditions as $AgInS_2$-ZnS solid solutions reveal that both the pure ZnS and $AgInS_2$ are irregular, well-dispersed nanoparticles. The inset of Figure 1b shows a typical TEM image of a single ZnS nanoparticle. We can identify two lattice fringes with spacing of 0.226 and 0.191 nm, which are very close to the inter-plane spacing of (102) and (110) planes, respectively, calculated from XRD data. Similarly, the two lattice fringes with spacings of 0.133 and 0.145 nm in the single $AgInS_2$ nanoparticle were observed, which are close to the inter-plane spacings of (332) and (400) planes, respectively (inset of Figure 1c). The corresponding fast Fourier transform (FFT) analysis of the pure $AgInS_2$ and ZnS nanoparticles also supports the above conclusion.

The representative low-magnification TEM image of the $AgInS_2$-ZnS solid solution nanorods is shown in **Figure 2**a. We can see that the nanorods exhibit high aspect ratio with noncentrosymmetric geometry and the distribution of nanorod lengths is relatively narrow. Aided by a statistical analysis of 200 nanorods, we determined the average length of nanorods to be 32 nm, with a standard deviation of ±5 nm,

NANO MICRO small

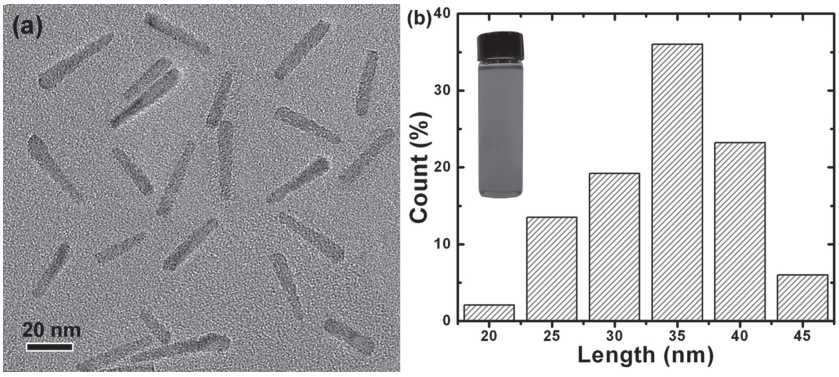

Figure 2. (a) TEM image of as-prepared $AgInS_2$-ZnS solid solution nanorods (x = 0.65) at low magnification and (b) length distributions of the solid solution nanorods. The inset in (b) is the photograph of $AgInS_2$-ZnS nanorods dispersed in chloroform solution, which forms a homogeneous, transparent suspension.

as shown in Figure 2b. The inset of Figure 2b shows that the resulting $AgInS_2$-ZnS solid solution nanorods can be well dispersed in chloroform to form homogeneous, transparent suspensions.

To investigate the structure of $AgInS_2$-ZnS solid solution nanorods, we analyzed an individual nanorod. The high-resolution TEM (HRTEM) image of the individual solid solution nanorod in **Figure 3**a revealed that the interplanar distance was 0.331 nm, which was close to the interplanar distance of the (010) plane of the bulk hexagonal structure of ZnS. It can be observed that the nanorods grew along the [100] orientation of ZnS as marked with an arrow shown in Figure 3a, which was also consistent with the FFT analysis of the nanorod (in the inset of Figure 3a). However, it is noticed that the crystal lattice pattern at the nanorod's larger end is not very clear. To fully understand the difference, we further analyzed the components at the two ends of the nanorod. The scanning transmission electron microscopy (STEM) image in Figure 3b shows an outline of the corresponding nanorod. The energy-dispersive X-ray spectroscopy (EDS) spectra in Figure 3c,d were taken from the two ends (Point A and Point B) of the nanorod. Although both of the two EDS spectra indicated the presence of Ag, In, Zn, and S elements in the sample, the ratio of $AgInS_2$ to ZnS was larger at Point A (Ag:In:Zn = 1:1:0.68) than that at Point B (Ag:In:Zn = 1:1:1.82), suggesting that the solid solution nanorods possessed a graded composition along their length. The higher $AgInS_2$ fraction at the larger end of the nanorod inferred the faster growth rate of $AgInS_2$ compared to ZnS. The observation is also supported by recent studies showing that the melting point of materials may influence their growth rate in solution to a certain extent and the materials with lower melting point tend to have faster growth rate.[58] In our case, this is consistent with the melting point of tetragonal $AgInS_2$ (880 ± 10 °C) is lower than that of wurtzite ZnS (1700 °C). During synthesis, in the beginning of the decomposition of $(AgIn)_xZn_{2(1-x)}(S_2CN(C_2H_5)_2)_4$, due to the faster growth rate of $AgInS_2$, more $AgInS_2$ formed than ZnS in the nanorod heads. This facilitated $AgInS_2$ not only to be substituted for ZnS on regular sites (substitutional) but also to take up spaces between regular sites (interstitial). As the growth of nanorods proceeded, the source of $AgInS_2$ would reduce dramatically while that of ZnS still maintained high concentration because of the relatively slow growth rate of ZnS, which increased ZnS fraction in solid solution nanorods, allowing $AgInS_2$ primarily to substitute for ZnS on their regular sites (inset of Figure 3d).

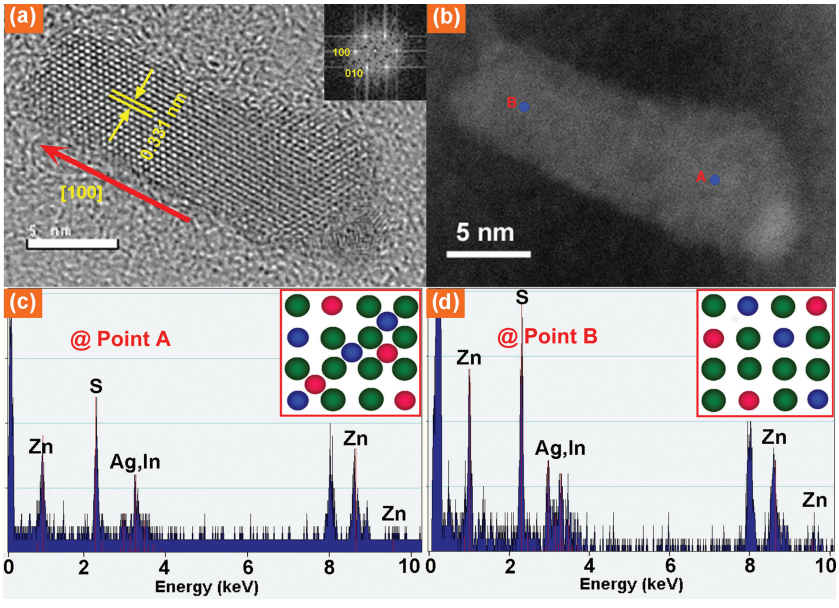

Figure 3. (a) Contrast-enhanced Fourier-filtered HRTEM images, (b) STEM image, and (c,d) EDS analysis of a single $AgInS_2$-ZnS solid solution nanorod (x = 0.65) at positions A and B, respectively. The inset in (a) is the FFT pattern of original HRTEM image along the [001] zone axis. The insets in (b) and (c) are the schemes of crystal structures of solid solutions. The green dots represent Zn element, the red dots represent Ag element, and the blue dots represent In element.

To reveal the formation mechanism of $AgInS_2$-ZnS solid solution nanorods, time-dependent morphological evolution experiments were performed by intercepting intermediate products in different reaction stages of 7, 12, 21, and 30 min. The resulting solid products were purified and imaged using TEM, as shown in **Figure 4**a-d. At the initial stage, the decomposition of $(AgIn)_xZn_{2(1-x)}(DDTC)$ (x = 0.65) at 200 °C quickly produced a large amount of $AgInS_2$-ZnS solid solution nuclei with high $AgInS_2$ fraction owing to the faster growth rate of $AgInS_2$ than ZnS. Subsequently, homogeneous $AgInS_2$-rich nanocrystals (nanorod heads) with an average diameter of 7 nm were obtained, serving as the starting seeds

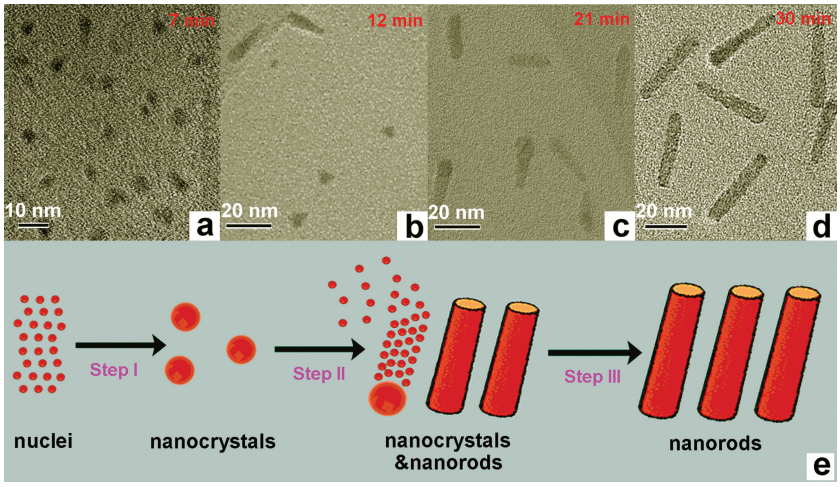

Figure 4. TEM images of $AgInS_2$-ZnS solid solution nanorods (x = 0.65). The synthesis times are a) 7 min, b) 12 min, c) 21 min, and d) 30 min. e) Schematic of the proposed mechanism for $AgInS_2$-ZnS solid solution nanorods.

(Figure 4a). Notably, these $AgInS_2$-rich nanorod heads are also solid solution maintaining the hexagonal structure of ZnS. At the second stage, a small amount of short nanorods with thin tails appeared at 12 min (Figure 4b). The elongation process of solid solution nanorods could be attributed to the heterogeneous nucleation of ZnS-rich solid solution tails depositing on the surface $AgInS_2$-rich solid solution seeds along the [100] direction. By the third stage, more nanorods emerged with only a small portion of nanoparticles remaining at 21 min (Figure 4c). Finally, the TEM image in Figure 4d revealed that the end product contained a large quantity of uniform nanorods with an average length of 32 nm. Based on the above TEM results together with the analysis of single nanorods, we proposed an anisotropic growth mechanism with different steps as depicted in Figure 4e: (1) fast nucleation and formation of $AgInS_2$-rich nanorod heads serving as the starting seeds, (2) heterogeneous nucleation and slow growth of a ZnS-rich thin tail on the seed surface, and (3) short nanorods further growing into longer nanorods. A similar growth mechanism on the synthesis of heterostructured CdS/CdSe nanorods with a certain degree of alloying has been recently reported by Vela et al.[58]

It is worth mentioning that the formation of nanorods strongly depends on the chemical composition of the $AgInS_2$-ZnS solid solutions. From the TEM images in **Figure 5**, it can be seen that the uniform nanorods can only be obtained when $AgInS_2$-ZnS solid solutions have appropriate compositions when the value of x is between 0.55 and 0.65 and the corresponding mole fraction of $AgInS_2$ in solid solution nanorods is approximately 38–48%.

The UV-vis absorption spectrum of the resulting $AgInS_2$-ZnS solid solution nanorods shows intense absorption bands with steep edges in the visible region and the onset of absorption edge was observed between those of ZnS and $AgInS_2$. The band gap of the solid solution nanorods is estimated to be 1.90 eV from the onset of the absorption edge. Furthermore, the photoluminescence spectrum (PL) of the $AgInS_2$-ZnS solid solution nanorods was measured at room temperature (**Figure 6**b). Compared to pure $AgInS_2$ and ZnS nanoparticles, a strong emission band centered at 680 nm can be observed from $AgInS_2$-ZnS solid solution nanorods (by 465 nm excitation), while there is almost no or weak emission from pure $AgInS_2$ or ZnS nanoparticles in the range examined. The onset of excitation spectrum is located at almost the same position as that of the corresponding absorption spectrum, which indicates that the emission of the $AgInS_2$-ZnS solid solution nanorods results from band gap excitation (Figure 6c). The inset shows an eye-visible photograph of the strong red photoluminescence from the solid solution nanorods excited under blue irradiation from a 465 nm lamp.

For the $AgInS_2$-ZnS solid solution nanorods, the optical properties have been found to be influenced by their composition. As shown in **Figure 7**, the absorption and emission spectra are both blue-shifted as the mole fraction of ZnS increases. The peak wavelength of PL was blue-shifted from 700 to 650 nm with decreasing *x* as shown in Figure 7b. The corresponding shift in the absorption spectra shown in Figure 7a was also observed here (it can be noted that the wavelength of optical absorption onset was not clearly identified when the mole fraction (x) of $AgInS_2$ in solid solution nanorods was less than 0.65). These observations show that the $AgInS_2$-ZnS solid solution nanorods are promising optical nanomaterials in which the energy band structure can be conveniently tuned. In addition, it is found that the

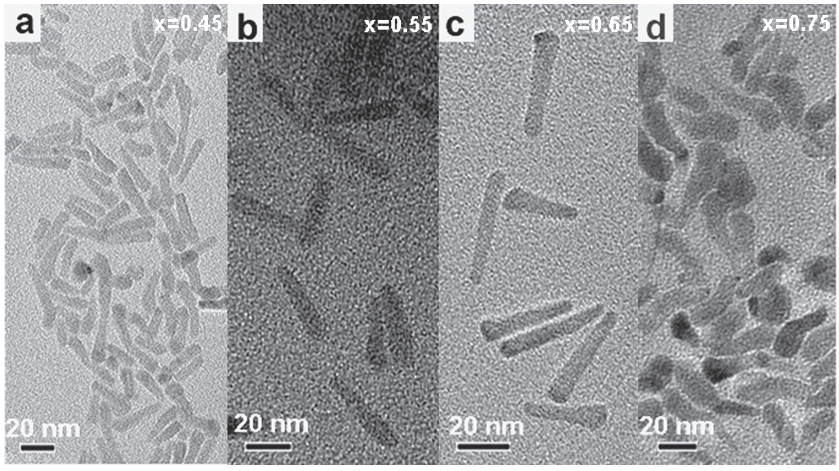

Figure 5. TEM images of as-prepared $AgInS_2$-ZnS solid solutions with a series of chemical compositions. The value of x in $(AgIn)_xZn_{2(1-x)}(S_2CN(C_2H_5)_2)_4$ used as a precursor is indicated in the figure.

small NANO MICRO

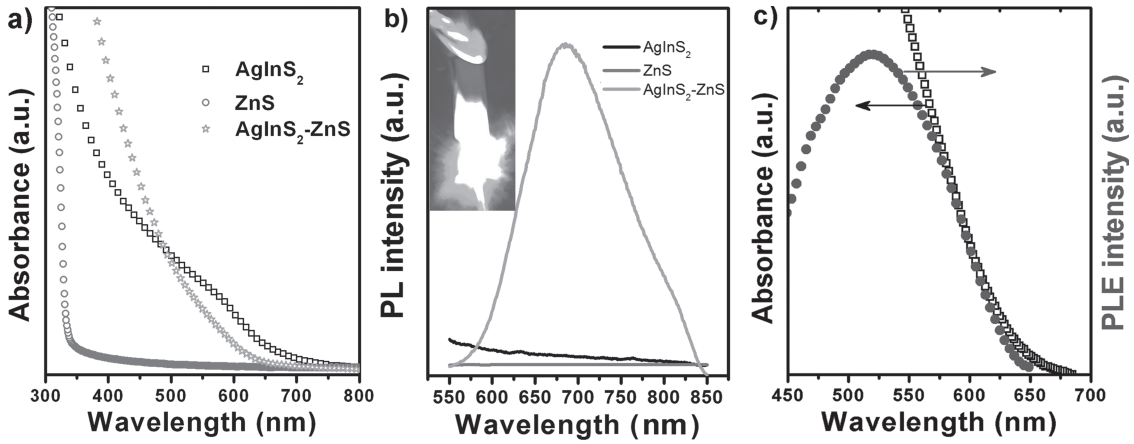

Figure 6. UV-vis absorption spectra (a) and photoluminescence spectra (b) of the $AgInS_2$-ZnS solid solution nanorods, $AgInS_2$ and ZnS nanoparticles synthesized at the same condition. The inset of Figure b shows an eye-visible photograph of the red photoluminescence from the $AgInS_2$-ZnS solid solution nanorods excited under blue irradiation using a 465 nm lamp. (c) UV-vis absorption spectra and photoluminescence excitation (PLE) of the $AgInS_2$-ZnS solid solution nanorods.

$AgInS_2$-ZnS solid solutions with uniform nanorod structure (for x = 0.55–0.65) yield much stronger luminescence. The maximum quantum yield (QY) value of these $AgInS_2$-ZnS solid solutions is 32.5%, which is better than that reported previously.[55] Also, the PL intensity of as-prepared $AgInS_2$-ZnS nanorod solution is almost constant for at least 3 months when stored under N_2 atmosphere.

In summary, we have demonstrated an efficient approach to synthesize soluble, narrowly dispersed $AgInS_2$-ZnS solid solution nanorods. This is the first demonstration of oriented growth for semiconductor solid solution nanorods via a one-pot solvothermal method. This anisotropic growth of $AgInS_2$-ZnS solid solution nanorods can be attributed to the different growth rates of their components (where the growth rate of $AgInS_2$ is much faster than ZnS). As a result, the $AgInS_2$-rich solid solution head segment is formed first, serving as the starting seeds. Over time, ZnS-rich thin tails slowly grow on the nanorod heads, forming the thin tail segments along the [100] direction. The morphology of the resulting $AgInS_2$-ZnS solid solutions strongly depends on their chemical composition and uniform solid solution nanorods are only obtained when the mole fraction of $AgInS_2$ in the solid solution nanorods is between 38 and 48%. The resulting nanorods exhibit high QY levels and tunable color, suggesting significant potential for lighting, biolabeling, and visible-light-driven photocatalyst applications. These results provide an efficient and convenient way to directly synthesize functional semiconductor solid solution nanorods. Although this study concerns the $AgInS_2$-ZnS system, we believe that this strategy can also be extended to other solid solution systems.

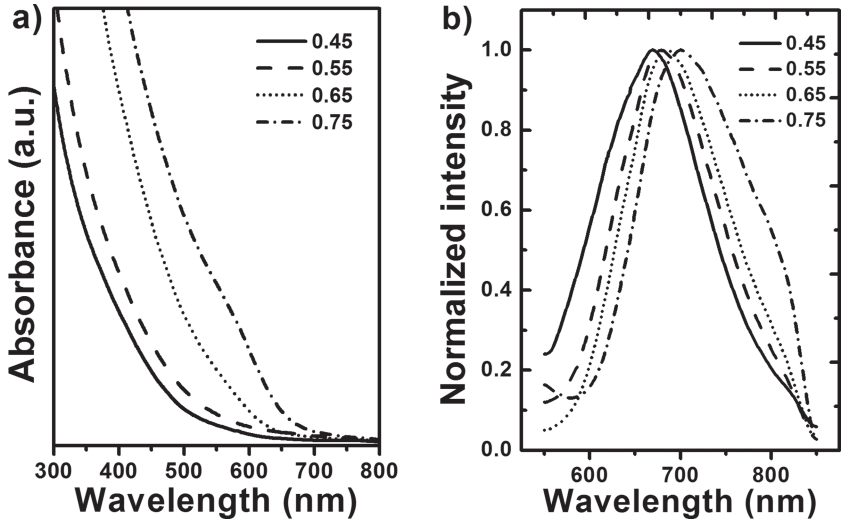

Figure 7. Absorption spectra (a) and normalized PL spectra (b) of $AgInS_2$-ZnS solid solutions prepared by decomposition of $(AgIn)_xZn_{2(1-x)}(S_2CN(C_2H_5)_2)_4$. The value of x is indicated in the figure.

Experimental Section

Chemicals: Oleic acid (OA; 90%, Aldrich), Octadecylamine (ODA; 90%, Aldrich), 1-Octadecene (ODE; 90%, Aldrich), $(C_2H_5)_2NCS_2Na{\cdot}3H_2O$ ((Na(DDTC); ACS reagent, Sigma-Aldrich), $AgNO_3$ (99.9+%, Alfa Aesar), $In(NO_3)_3$ (99.9%, Aldrich), $Zn(NO_3)_2$ (99%, Sinopharm Chemical Reagent Co., Ltd), ethanol (AR), chloroform (AR). All chemicals were used as received without further purification. The $AgInS_2$-ZnS solid solution nanorods were synthesized by using standard air-free procedures.

Synthesis of Monodisperse $AgInS_2$-ZnS Nanorods: A typical procedure is given as follows: 50 mg of $(AgIn)_xZn_{2(1-x)}$(DDTC) was added into the solvent made of 10 mmol of OA, 10 mmol of ODA, and 20 mmol of ODE in a three-necked flask (50 mL) at room temperature. Subsequently, the slurry was heated to

100 °C to remove water and oxygen with vigorous magnetic stirring under vacuum for several minutes in a temperature-controlled electromantle to form an optically transparent solution. The solution was then heated to 200 °C at a heating rate of 15 °C/min and kept for 30 min under Ar atmosphere. After cooling down to room temperature, the solid solution nanorods were precipitated by adding an excess amount of the absolute ethanol into the reacted solution, followed by washing with ethanol and drying in oven at 80 °C. The resulting nanorods were easily re-dispersed in various nonpolar organic solvents (e.g., chloroform). The yield of nanorods was about 68–80%. The precursor $(AgIn)_xZn_{2(1-x)}(S_2CN(C_2H_5)_2)_4$ was prepared using the method introduced in ref [55].

Instrumentation: The powder X-ray diffraction (XRD) patterns of the as-prepared products were recorded on a Shimadzu 6000 X-ray diffractometer equipped with Cu Kα radiation ($\lambda = 1.5405$ Å). Samples for transmission electron microscopy (TEM) and scanning transmission electron microscopy (STEM) analyses were prepared by drying a drop of nanorod dispersion in chloroform on amorphous carbon-coated copper grids. High-resolution TEM (HRTEM) characterization was performed with a transmission electron microscope (JEOL, JEM-2010) operating at 200 kV. STEM measurements were performed using an FEI Titan STEM, with Schottky Field Emission Gun (FEG), operated at 200 kV. EDX spectra were acquired in STEM mode using a probe size of around 1 nm, with an acquisition time of 20 s, while scanning the STEM probe over a small area of around 4 nm by 4 nm, to minimize damage to the material during EDX acquisition. The photoluminescence (PL) and photoluminescence excitation (PLE) spectra were recorded in the spectral range of 350–850 nm at room temperature using a 450 W xenon lamp as the excitation source. The absorption spectra were obtained over a wavelength range from 300 to 800 nm using a UV-vis spectrophotometer (Shimadzu) with a 50 W halogen lamp and a deuterium lamp as the excitation source. The PL QY of $AgInS_2$-ZnS nanorods was measured by comparing the integrated area of photoluminescence emission of rhodamine 6G in ethanol (QY = 95%) with $AgInS_2$-ZnS nanorods in chloroform, with the same absorbance value at the excitation wavelength and similar fluorescence wavelength.

Acknowledgements

*The authors would like to thank the financial support from Singapore NRF-RF-2009-09, NRF-CRP-2011-02 and the Science and Engineering Research Council, Agency for Science, Technology and Research (A*STAR) of Singapore (project No. 092 101 0057). The work is also supported by the National Natural Science Foundation of China (NSFC) (project Nos. 61006037 and 61076015). Technical assistance from Mr. Yee Yan and Ms. Jun Guo are gratefully acknowledged.*

[1] W. U. Huynh, J. J. Dittmer, A. P. Alivisatos, *Science* **2002**, *295*, 2425–2427.
[2] D. V. Talapin, R. Koeppe, S. Götzinger, A. Kornowski, J. M. Lupton, A. L. Rogach, O. Benson, J. Feldmann, H. Weller, *Nano Lett.* **2003**, *3*, 1677–11681.
[3] A. Rizzo, C. Nobile, M. Mazzeo, M. D. Giorgi, A. Fiore, L. Carbone, R. Cingolani, L. Manna, G. Gigli, *ACS Nano* **2011**, *3*, 1506–1512.
[4] A. E. Saunders, A. Ghezelbash, P. Sood, B. A. Korgel, *Langmuir* **2008**, *24*, 9043–9049.
[5] L. S. Li, A. P. Alivisatos, *Phys. Rev. Lett.* **2003**, *90*, 097402–097403.
[6] A. Ghezelbash, B. Koo, B. A. Korgel, *Nano Lett.* **2006**, *6*, 1832–1836.
[7] H. Steinberg, O. Wolf, A. Faust, A. Salant, Y. Yigal Lilach, O. Millo, U. Banin, *Nano Lett.* **2010**, *10*, 2416–2420.
[8] X. W. Xie, Y. Li, Z. Q. Liu, M. Haruta, W. J. Shen, *Nature* **2009**, *458*, 746–749.
[9] M. C. Newton, S. J. Leake, R. Harder, I. K. Robinson, *Nat. Mater.* **2010**, *9*, 120–124.
[10] J. D. Doll, G. S. Pilania, R. Ramprasad, F. Papadimitrakopoulos, *Nano Lett.* **2010**, *10*, 680–685.
[11] H. Lange, M. Mohr, M. Artemyev, U. Woggon, C. Thomsen, *Nano Lett.* **2008**, *8*, 4614–4617.
[12] S. P. Ahrenkiel, O. I. Mićić, A. Miedaner, C. J. Curtis, J. M. Nedeljković, A. J. Nozik, *Nano Lett.* **2003**, *3*, 833–837.
[13] Z. B. Zhuang, X. T. Lu, Q. Peng, Y. D. Li, *J. Am. Chem. Soc.* **2010**, *132*, 1819–1821.
[14] B. Sadtler, D. O. Demchenko, H. M. Zheng, S. M. Hughes, M. G. Merkle, U. Dahmen, L. W. Wang, A. P. Alivisatos, *J. Am. Chem. Soc.* **2009**, *131*, 5285–5293.
[15] C. O'Sullivan, R. D. Gunning, A. Sanyal, C. A. Barrett, H. Geaney, F. R. Laffir, S. Ahmed, K. M. Ryan, *J. Am. Chem. Soc.* **2009**, *131*, 12250–12257.
[16] F. D. Wang, W. E. Buhro, *J. Am. Chem. Soc.* **2007**, *129*, 14381–14387.
[17] M. T. Ng, C. B. Vittal, J. J. Boothroyd, *J. Am. Chem. Soc.* **2006**, *128*, 7118–7119.
[18] X. Sheng, L. Wang, L. Chang, Y. Luo, H. Zhang, J. Wang, D. Yang, *Chem. Commun.* **2012**,*48*, 4746–4748.
[19] T. Mirkovic, D. Rossouw, G. A. Botton, G. D. Scholes, *Chem. Mater.* **2011**, *23*, 181–187.
[20] A. Sitt, A. Salant, G. Menagen, U. Banin, *Nano Lett.* **2011**, *11*, 2054–2060.
[21] A. A. Lutich, C. Mauser, E. D. Como, J. Huang, A. Vaneski, D. V. Talapin, A. L. Rogach, J. Feldmann, *Nano Lett.* **2010**, *10*, 4646–4650.
[22] G. X. Zhu, Z. Xu, *J. Am. Chem. Soc.* **2011**, *133*, 148–157.
[23] X. H. Li, J. Lian, M. Lin, Y. Chan, *J. Am. Chem. Soc.* **2011**, *133*, 672–675.
[24] N. Sharma, X. Guo, G. Du, Z. Guo, J. Wang, Z. Wang, V. K. Peterson, *J. Am. Chem. Soc.* **2012**, *134*, 7867–7873.
[25] Y. Nagaoka, T. Wang, J. Lynch, D. La Montagne, Y. C. Cao, *Small* **2012**, *8*, 843–846.
[26] S. P. Lau, L. Huang, S. F. Yu, H. Yang, J. K. Yoo, S. J. An, G.-C. Yi, *Small* **2006**, *2*, 736–740.
[27] T. Xu, C. Lin, C. Wang, D. L. Brewe, Y. Ito, J. Lu, *J. Am. Chem. Soc.* **2010**, *132*, 2151–2153.
[28] K. Kusada, M. Yamauchi, H. Kobayashi, H. Kitagawa, Y. Kubota, *J. Am. Chem. Soc.* **2010**, *132*, 15896–15898.
[29] D. F. Wang, T. Kako, J. H. Ye, *J. Am. Chem. Soc.* **2008**, *130*, 2724–2725.
[30] B. Ellis, L. K. Perry, D. H. Ryan, L. F. Nazar, *J. Am. Chem. Soc.* **2006**, *128*, 11416–11422.
[31] O. Mentré, E. M. Ketatni, M. Colmont, M. Huvé, F. Abraham, V. Petricek, *J. Am. Chem. Soc.* **2006**, *128*, 10857–10867.
[32] K. Maeda, T. Takata, M. Hara, N. Saito, Y. Inoue, H. Kobayashi, K. Domen, *J. Am. Chem. Soc.* **2005**, *127*, 8286–8287.
[33] X. Liang, X. Wang, Y. Zhuang, B. Xu, S. M. Kuang, Y. D. Li, *J. Am. Chem. Soc.* **2008**, *130*, 2736–2737.
[34] Y. Huang, Z. Zheng, Z. H. Ai, L. Zhang, X. Fan, Z. Zou, *J. Phys. Chem. B* **2006**, *110*, 19323–19328.
[35] X. Liang, X. Wang, Y. Zhuang, B. Xu, S. Kuang, Y. Li, *J. Am. Chem. Soc.* **2008**, *130*, 2736–2737.

[36] T. Erdem, H. V. Demir, *Nat. Photonics* **2011**, *5*, 126.
[37] Y. D. Jin, X. H. Gao, *Nat. Nanotechnol.* **2009**, *4*, 571–576.
[38] U. O. S. Seker, T. Ozel, H. V. Demir, *Nano Lett.* **2011**, *11*, 1530–1539.
[39] A. J. N. Bader, A. A. Ilkevich, I. V. Kosilkin, J. M. Leger, *Nano Lett.* **2011**, *11*, 461–465.
[40] G. M. Wang, X. Y. Yang, F. Qian, J. Z. Zhang, Y. Li, *Nano Lett.* **2010**, *10*, 1088–1092.
[41] Z. Li, X. G. Peng, *J. Am. Chem. Soc.* **2011**, *133*, 6578–6586.
[42] H. S. Kim, N. C. Jeong, K. B. Yoon, *J. Am. Chem. Soc.* **2011**, *133*, 1642–1645.
[43] H. V. Demir, U. O. S. Seker, G. Zengin, E. Mutlugun, E. Sari, C. Tamerler, M. Sarikaya, *ACS Nano* **2011**, *5*, 2735–2741.
[44] R. Chen, M. I. B. Utama, Z. P. Peng, B. Peng, Q. H. Xiong, H. D. Sun, *Adv. Mater.* **2011**, *23*, 1404–1408.
[45] J. H. Bang, P. V. Kamat, *Adv. Funct. Mater.* **2010**, *20*, 1970–1976.
[46] D. Grodzińska, W. H. Evers, R. Dorland, J. Rijssel, M. A. Huis, A. Meijerink, C. M. Donegá, D. Vanmaekelbergh, *Small* **2011**, *7*, 3493–3501.
[47] Z. He, J. Jie, W. Zhang, W. Zhang, L. Luo, X. Fan, G. Yuan, I. Bello, S.-T. Lee, *Small* **2009**, *5*, 345–350.
[48] L. Li, A. Pandey, D. J. Werder, B. P. Khanal, J. M. Pietryga, V. I. Klimov, *J. Am. Chem. Soc.* **2011**, *133*, 1176–1179.
[49] R. Xie, M. Rutherford, X. Peng, *J. Am. Chem. Soc.* **2009**, *131*, 5691–5697.
[50] X. Gou, F. Cheng, Y. Shi, L. Zhang, S. Peng, J. Chen, P. Shen, *J. Am. Chem. Soc.* **2006**, *128*, 7222–7229.
[51] J. Zhang, R. Xie, W. Yang, *Chem. Mater.* **2011**, *23*, 3357–3361.
[52] L. Li, T. J. Daou, I. Texier, T. T. K. Chi, N. Q. Liem, P. Reiss, *Chem. Mater.* **2009**, *21*, 2422–2429.
[53] B. Mao, C.-H. Chuang, J. Wang, C. Burda, *J. Phys. Chem. C* **2011**, *115*, 8945–8954.
[54] I. Tsuji, H. Kato, H. Kobayashi, A. Kudo, *J. Am. Chem. Soc.* **2004**, *126*, 13406–13413.
[55] T. Torimoto, T. Adachi, K.-I. Okazaki, M. Sakuraoka, T. Shibayama, B. Ohtani, A. Kudo, S. Kuwabata, *J. Am. Chem. Soc.* **2007**, *129*, 12388–12389.
[56] T. Torimoto, S. Ogawa, T. Adachi, T. Kameyama, K.-I. Okazaki, T. Shibayama, A. Kudo, S. Kuwabata, *Chem. Commun.* **2010**, *46*, 2082–2084.
[57] T. Sasamura, K.-I. Okazaki, R. Tsunoda, A. Kudo, S. Kuwabata, T. Torimoto, *Chem. Lett.* **2010**, *39*, 619–621.
[58] T. P. A. Ruberu, J. Vela, *ACS Nano* **2011**, *5*, 5775–5784.

Received: October 28, 2012
Published online: April 16, 2013